SLAS Discovery 28 (2023) 211–222

Contents lists available at ScienceDirect

SLAS Discovery

journal homepage: www.elsevier.com/locate/slasd

Original Research

Fluorescent probe for the identification of potent inhibitors of the macrophage infectivity potentiator (Mip) protein of *Burkholderia pseudomallei*

Nicolas Julian Scheuplein[a,‡], Theresa Lohr[a,‡], Mirella Vivoli Vega[b,¶], Dyan Ankrett[b], Florian Seufert[a], Lukas Kirchner[a], Nicholas J. Harmer[b,*], Ulrike Holzgrabe[a,*]

[a] *Institute of Pharmacy and Food Chemistry, University of Würzburg, Am Hubland, Würzburg 97074, Germany*
[b] *Living Systems Institute, Stocker Road, Exeter EX4 4QD, UK*

ARTICLE INFO

Keywords:
PPIase
Fluorescence polarization
Anisotropy
High throughput screening
Burkholderia pseudomallei Mip
Mip inhibitor

ABSTRACT

The macrophage infectivity potentiator (Mip) protein belongs to the immunophilin superfamily. This class of enzymes catalyzes the interconversion between the *cis* and *trans* configuration of proline-containing peptide bonds. Mip has been shown to be important for the virulence of a wide range of pathogenic microorganisms, including the Gram-negative bacterium *Burkholderia pseudomallei*. Small molecules derived from the natural product rapamycin, lacking its immunosuppression-inducing moiety, inhibit Mip's peptidyl-prolyl *cis-trans* isomerase (PPIase) activity and lead to a reduction in pathogen load *in vitro*. Here, a fluorescence polarization assay (FPA) to enable the screening and effective development of BpMip inhibitors was established. A fluorescent probe was prepared, derived from previous pipecolic scaffold Mip inhibitors labeled with fluorescein. This probe showed moderate affinity for BpMip and enabled a highly robust FPA suitable for screening large compound libraries with medium- to high-throughput (Z factor ~ 0.89) to identify potent new inhibitors. The FPA results are consistent with data from the protease-coupled PPIase assay. Analysis of the temperature dependence of the probe's binding highlighted that BpMip's ligand binding is driven by enthalpic rather than entropic effects. This has considerable consequences for the use of low-temperature kinetic assays.

Introduction

The macrophage infectivity potentiator (Mip) protein has emerged as a promising new anti-virulence target in the effort to find new treatments for bacteria that display either intrinsic or acquired resistance to antimicrobials [1–4]. Mip proteins are found across Gram-negative bacteria and in some unicellular parasites. They have been associated with virulence in proteobacteria (e.g. *Legionella* [5], *Burkholderia* [2], *Klebsiella* [3], and *Neisseria* [6]), other Gram-negative pathogens such as *Chlamydia* [7,8], and eukaryotic pathogens (trypanosoma [9] and leishmania [3]). Mips consist of a highly conserved FKBP type pre-prolyl peptide isomerase (peptidyl-prolyl isomerase, PPIase) domain, and in most cases one of two dimerization/chaperone domains. The PPIase domain has the greatest contribution to virulence, and can be inhibited by small molecules, leading to a decrease in pathogen load *in vitro* [4]. One such targetable pathogen is *Burkholderia pseudomallei*, the causative agent of

Abbreviations: ATR, attenuated total reflectance; Boc, *tert*-butyloxycarbonyl; BpMip, *Burkholderia pseudomallei* Mip; C18, octyldecylsilane; Cbz, benzyl chloroformate; DAD, diode array detection; DCC, *N,N′*-dicyclohexylcarbodiimide; DCM, dichloromethane; DIPEA, *N,N*-diisopropylethylamine; DMAP, 4-dimethylaminopyridine; DMF, dimethylformamide; DMSO, dimethyl sulfoxide; EA, ethyl acetate; EDC-HCl, 1-ethyl-3-(3-dimethylaminopropyl)carbodiimide hydrochloride; ELSD, evaporative light scattering detector; FA, formic acid; FKBP, FK506 binding proteins; FP, fluorescence polarization; FPA, fluorescence polarization assay; HBTU, hexafluorophosphate benzotriazole tetramethyl uronium; HOBt, 1-hydroxybenzotriazole; HPLC, high performance liquid chromatography; HRMS, high-resolution mass spectrometry; HTS, high-throughput screening; IC_{50}, inhibitory concentration of 50%; IR, infrared; K_D, dissociation constant; K_i, inhibition constant; λ_{max}, lambda max, wavelength at which a substance has its strongest photon absorption; Mip, macrophage infectivity potentiator; mP, millipolarization; NEt_3, triethylamine; NMR, nuclear magnetic resonance; PDB ID, Protein Data Bank Identification; PE, petroleum ether; PPIase, peptidyl-prolyl *cis-trans* isomerase; rt, room temperature; SAR, structure–activity relationships; TFA, trifluoroacetic acid; TLC, thin layer chromatography.

* Corresponding authors.
E-mail addresses: N.J.Harmer@exeter.ac.uk (N.J. Harmer), ulrike.holzgrabe@uni-wuerzburg.de (U. Holzgrabe).
‡ equal first authors.
¶ Present address: School of Biochemistry, University of Bristol, Bristol BS8 1TD, UK.

https://doi.org/10.1016/j.slasd.2023.03.004
Received 24 January 2023; Received in revised form 2 March 2023; Accepted 20 March 2023
Available online 29 March 2023

melioidosis [10]. This potentially life-threatening infection causes an estimated global burden of 84.3 per 100 000 people or 4.6 million disability-adjusted life years per year [11]. *B. pseudomallei* is a Gram-negative betaproteobacterium containing two Mip paralogues. Of these, only the 11.9 kDa BpMip protein (consisting of only a PPIase domain) is relevant to virulence [2,12]. BpMip shows 40% sequence identity to the *Legionella pneumophila* Mip [13,14], with almost identical active sites [2].

For the targeted development of new inhibitors, rapid and robust measurement of binding affinity is crucial. In the past, Mip inhibitors designed by Juli et al. [15,16] and Seufert et al. [17,18] have been screened using a protease-coupled PPIase assay established by Fischer et al. [19] Briefly, a short amino acid sequence labeled with *p*-nitroaniline is used as a substrate, while α-chymotrypsin serves as an auxiliary protease that cleaves only trans-linked Phe-Pro substrates. The conversion can be measured by absorbance at around 390 nm, which is due to the released *p*-nitroaniline [19]. This assay has some disadvantages as it has to be carried out at low temperatures, making it time-consuming and requiring dedicated equipment. [20,21] Whilst the PPIase assay directly measures the desired effect of proposed inhibitors, it is highly challenging to use for high-throughput screening (HTS).

A fluorescence polarization (FP) assay could be a potent alternative for HTS. FP uses plane-polarized light to measure the binding of a small fluorescent ligand to a larger protein, detecting the change in the effective molecular volume. [22,23] The FP assay (FPA) has significant advantages compared to other assays used to study enzyme-ligand interactions for studying the Mip-ligand interaction [24]. It does not require separation of bound and free ligand, allowing ligand binding to be quantified without disturbing the equilibrium. This makes it suitable for measuring interactions with low affinity and rapid dissociation rates, such as the Mip-ligand interaction [23]. FP avoids the use of radioactivity, is non-destructive, and can resolve thermodynamic parameters such as ΔH° and ΔS°, requiring less protein than an isothermal titration calorimetry measurement [23]. A key advantage for Mips is that FP can operate across temperatures where the sample protein is folded. This avoids the need to use low temperatures (as in the PPIase enzyme assay [19,20]), and can readily measure activity at 37°C, the relevant physiological conditions for human pathogens. Protein-ligand interactions can be highly temperature dependent, and lower temperature determinations can be misleading. Once established, the FPA can be performed in 384 or even 1536 well format with moderate read times, allowing for medium- or even high-throughput screening. Kozany et al. described the application of an FPA for the high-throughput screening of human FKBPs that show strong structural similarity to the microbial Mip PPIase domain [25]. Pomplun et al. used a refined FPA to screen compounds against microbial Mips, such as *Neisseria meningitidis* Mip (NmMip) [26]. However, the binding affinity of the tracer molecule previously used is very high (low nanomolar). This makes differentiation of weaker BpMip inhibitors in the competition assay more challenging. For initial screening aiming at obtaining compounds with a K_D of 1–10 μM, a tracer molecule binding in the low micromolar range would be a useful alternative. Furthermore, no application toward BpMip has been described to date.

Here, we describe the design of a fluorescent probe with a low micromolar affinity for the PPIase domain of the BpMip protein. We used this to establish a highly robust FPA suitable for medium to high throughput screening of large compound libraries to identify potent new inhibitors. We demonstrate the use of the assay to prioritize example compounds from our optimization pipeline for Mip inhibitors. This assay will facilitate and accelerate the search for new BpMip inhibitors and thus new therapeutic options against melioidosis and other microbial diseases caused by Mip-bearing pathogens. The analysis of the temperature dependence of the binding of the probe demonstrated that binding of this compound series is driven by enthalpic rather than entropic effects. Nevertheless, the temperature dependence is considerable. This has important consequences for the use of kinetic assays at low temperatures, as the compound affinity is expected to increase as the temperature lowers. The FPA presented here, which is performed at room temperature and could operate at 37°C, should therefore provide more valid and realistic results than the cooled protease-coupled PPIase assay.

Results and discussion

Design of tracer molecule 1

Key steps in probe design include the selection of a ligand to be labeled, as well as a suitable attachment point for a linker of appropriate length and a suitable fluorophore. These must not result in a significant loss of binding affinity due to steric hindrance [27]. The functionalized 5-carboxyfluorescein derivative was chosen as a fluorophore as it has similar properties to the parent compound fluorescein (Fig. 1). Fluorescein, being used in immunofluorescence microscopy [28] and various biochemical applications, [29,30] has excellent fluorescence properties for FP application, such as a high fluorescence quantum yield $\Phi = 0.92 \pm 0.02$ of the dianion form and a relatively long fluorescence lifetime of approximately 4 ns [31]. A similar fluorophore was used successfully in FP assays by Hausch et al. and Banaszynski et al. to screen potential FKBP ligands. [25,32] The absorption maximum λ_{max} for fluorescein lies at approximately 485 nm, sufficiently high to avoid autofluorescence of the sample, and its emission maximum λ_{em} is about 520 nm. [33,34] The coupling of the fluorescent dye to the ligand should be rigid enough so that the fluorophore cannot rotate independently of the status of the ligand, arguing against linkers that are too long [34]. A chain that is too short, on the other hand, can sterically hinder the binding of the inhibitor to the Mip protein. Banaszynski et al. showed that direct fluorescein labeling of rapamycin to the alcohol group of C40 significantly reduced binding to FKBP12 (K_D = 10 mM) [32]. By varying the linker length of their FP tracer for the screening of the related FKBP51 binding ligands, Hausch et al. found that a fluorescein-labeled tracer linked to rapamycin via glycine did not work for FKBP51, while a hexyl-glycine linker consisting of a total of eleven atoms proved to be suitable [25]. The small molecule FP tracer later used, being much smaller than rapamycin, worked successfully with a shorter chain length of only five atoms [25]. Based on the similarity of the binding pocket of human FKBPs and microbial Mips, a hexyl linker with a total length of ten atoms was selected (Fig. 1).

The crystal structures of BpMip bound to compound **2** (**SF354**, PDB ID 5V8T; Fig. 2A) [3] and **3** (**CJ168**, PDB ID 4G50; Fig. 2B) [16] highlight a likely point to introduce the linker without interfering in compound binding to BpMip. The pipecolic ring of both Mip inhibitors is located deep in the active site pocket, and the phenyl ring of the sulfonamide moiety occupies a sub-pocket, ruling out these parts of the molecule as a linkage point (Fig. 2). However, the trimethoxyphenyl group in the case of **3** and the ether-substituted benzene ring in the case of **2** are located rather superficially on the protein surface, rendering this part of the inhibitors an interesting linkage point (Fig. 2). Indeed, this group changes location in crystal structures with different protein packing, indicating that the interactions with Mip are weak [3]. The lead structure **2** has a $K_{i\ (PPIase)}$ of 0.98 ± 0.29 μM, despite carrying rather bulky ether groups that are well tolerated at this position [18]. Consequently, the attachment point for the linker was chosen in the *para* position on this benzene ring. The backbone of **2** was used for the Mip inhibitor moiety of the tracer, leaving out the ether groups at the benzene ring to prevent interactions with the fluorophore or the linker and to improve synthetic accessibility.

Synthesis of tracer 1

The primary amino group of 4-(aminomethyl)benzoic acid was Cbz-protected (to give **4**) and the acid function amide-coupled with ethanolamine using EDC-HCl and HOBt (Fig. 3). **5** was then esterified with *N*-Boc-(*S*)-pipecolic acid under Steglich conditions using DCC and

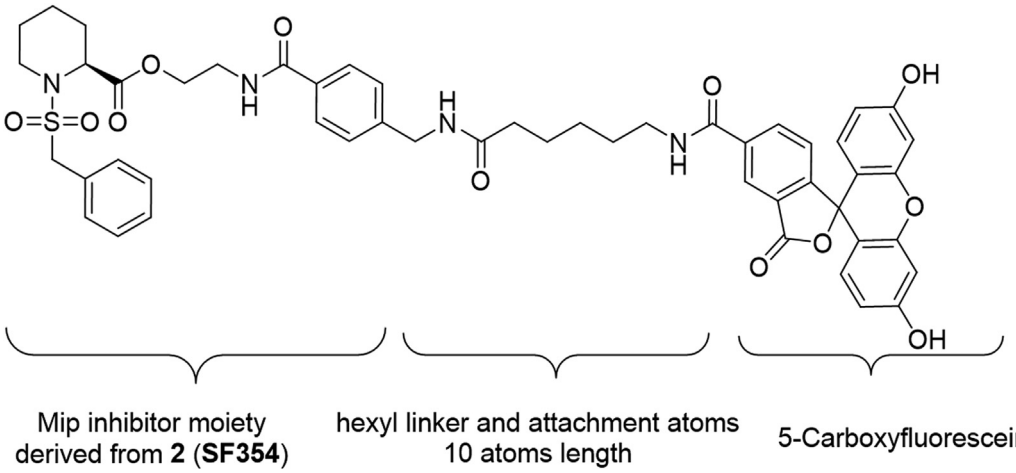

Fig. 1. Chemical structure of the designed FP tracer molecule **1**, consisting of a Mip inhibitor moiety derived from **2**, a hexyl linker and attachment atoms with a total length of 10 atoms, and the fluorophore 5-carboxyfluorescein.

catalytic amounts of DMAP. Subsequently, the Boc protecting group of **6** was cleaved with TFA, and the resulting amine **7** was coupled with phenylmethanesulfonyl chloride to give sulfonamide **8**. The Cbz protecting group was removed hydrogenolytically under Pd catalysis to obtain the primary amine **9**. The fluorophore linker moiety **10** was prepared by the reaction of 5-carboxyfluorescein with 6-methoxy-6-oxohexane-1-aminium chloride, the coupling reagent HBTU and NEt_3 in DMF followed by saponification of the methoxy ester with aqueous LiOH solution. In the final step, **9** was amide-coupled with **10** using HBTU and DIPEA to give tracer molecule **1**.

FP assay validation with BpMip and probe 1 and thermodynamic study of the influence of temperature on K_D

To establish the FP assay, the optimal concentration of tracer molecule **1** was determined by using different tracer concentrations when titrating the active site of BpMip.

To prove that fluorescence polarization is a concentration-independent parameter, **1** was subjected to a sensitivity test. By measuring a dilution series of the tracer molecule, we found that the tracer exhibits a stable polarization signal at concentrations ranging from 50 nM to 0.5 nM (Fig. 4A).

A concentration of 5 nM **1** gave strong fluorescence and reproducible results and was used for all further experiments. We firstly determined the affinity of **1** for purified BpMip (Fig. 4B). At 25°C, the affinity was 1200 ± 120 nM, which met our criteria for the intended affinity for BpMip. Based on this binding curve, a protein concentration of 2 μM was chosen for further experiments. Reviews of FP recommend using a concentration showing 50-80% of the plateau FP change, and a substantial polarization range. [35,36] A concentration of 2 μM provided high sensitivity to the competitor and offered a dynamic range of 70 mP, sufficient for precise calculations. We used a value giving slightly greater than a 50% response to account for the reduced affinity in the presence of DMSO. BpMip can be readily produced in sufficient quantities [37].

We then tested the affinity across a range of temperatures from 25°C to 55°C. The interaction showed a linear van't Hoff plot (Fig. 4C), suggesting that the heat capacity of the protein is unaffected by temperature. From the van't Hoff plot, the enthalpy (ΔH°) and entropy (ΔS°) were calculated as -44 ± 3 kJ mol^{-1} and -39 ± 11 J mol^{-1}, respectively [23]. Due to the negative entropic element, the K_D increased with temperature. Screening at higher temperatures would require greater concentrations of BpMip, compromising the economy and sensitivity of the experiment. This indicates that the compound would be most useful at 20–25°C, depending on the capabilities of the instrument. All further experiments were performed at room temperature with 2 μM BpMip.

A time-dependent equilibrium study was performed to investigate the stability of the enzyme-ligand complex formed. The formation occurred within the first few minutes and was stable for at least three hours (Fig. 5A). No significant difference was observed in the K_D between the first measurement a few minutes after setup to the last one after three hours.

Many screening compounds are only soluble in a carrier such as DMSO. DMSO is a common and bio-tolerated solvent for experimental compounds. However, it is well documented to affect protein-ligand binding [38]. Therefore, the effects of DMSO on the Mip-**1** complex were investigated in a DMSO tolerance assay [38]. An active site titration was performed in the presence of a defined DMSO concentration, and the change in binding capacity of the tracer was determined using the K_D value (Fig. 5B). DMSO showed a clear effect on BpMip's affinity for the fluorescent ligand. For higher DMSO concentrations, the minimum significance ratio (MSR = $10^{2\sqrt{2}s}$) of the K_D values relative to 0 % DMSO was calculated [39]. Using the common criterion of an MSR of less than 3, there was a significant difference at 10 % (v/v) DMSO. Although the MSR for DMSO concentrations of 5% or lower is less than 3, and so do not meet the test of a significant difference, the apparent K_D value already doubles at 1% (v/v) DMSO. To maintain a sufficient signal-to-noise ratio and maximum precision in the competition assay, an expedient DMSO limit was set at < 1% for the further experiments. This could be implemented because all inhibitors were sufficiently soluble in 1% (v/v) DMSO at the final assay concentration and is consistent with most HTS compounds [40]. **1** therefore satisfied our criteria as a useful tracer for moderate BpMip inhibitors and a good complement to the already known FKBP and Mip tracers. [25,26]

The assay was further validated by determining the binding affinity of probe **1** for BpMip using the gold standard isothermal titration calorimetry (ITC). The ITC experiment was performed in 3% (v/v) DMSO. The determined K_D of 5.50 ± 0.03 μM (Fig. 5C, Supplementary Fig. 3) shows good agreement with the FP assay (K_D = 3.63 μM at 3% DMSO). Furthermore, ITC determined the stoichiometry of the probe for BpMip as 1.10 ± 0.03, confirming that BpMip has only one binding site for probe **1**, and that the BpMip sample has good integrity and is at the determined concentration.

Finally, the specificity of the assay was investigated. The mixture of BpMip and labeled probe **1** was titrated against the unlabeled probe **8**, to demonstrate that FP decreases to a minimum with increasing concentration of competitor [35]. The similar K_D values of the two molecules show that labeling has no significant effect on Mip binding, confirming the approach of determining the attachment point from the crystal structures (Fig. 2).

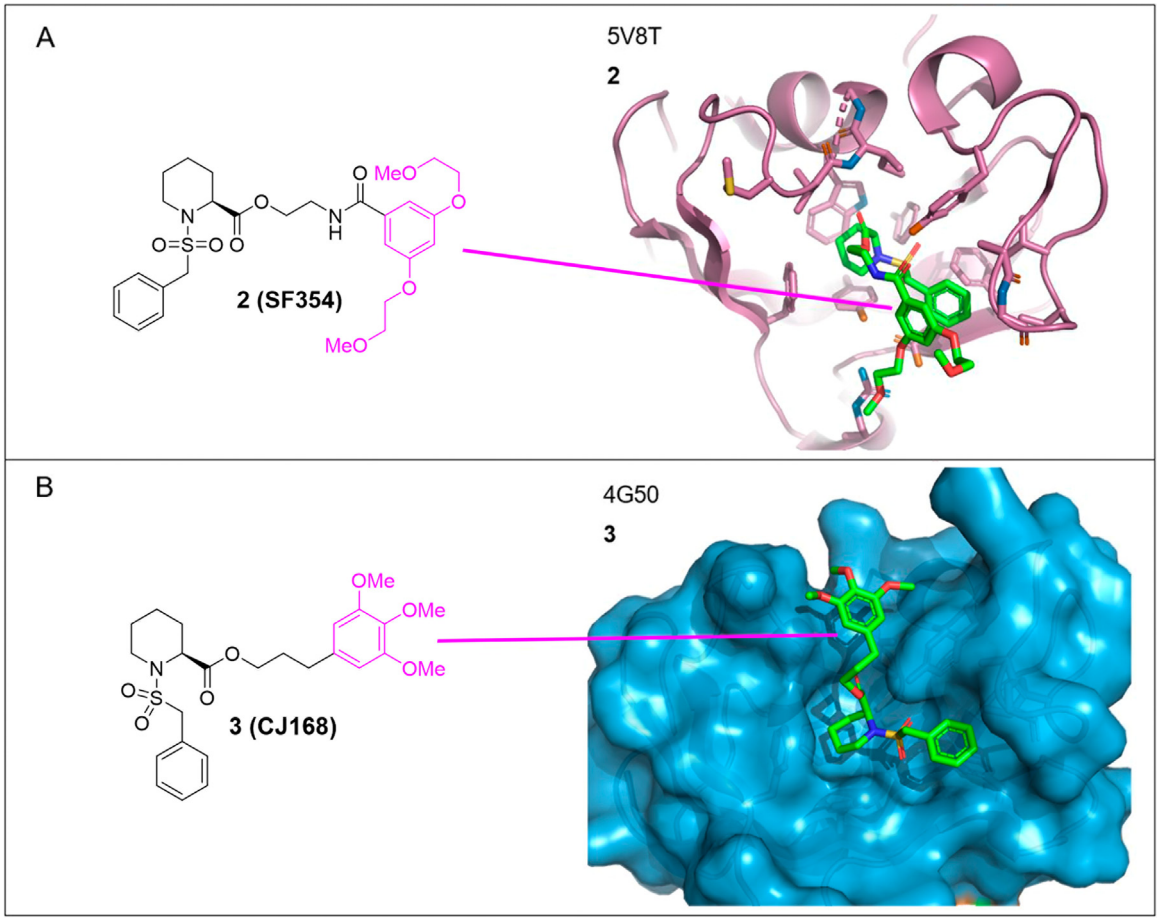

Fig. 2. Chemical structures of the Mip inhibitors **2** (Fig. 2A) and 3 (Fig. 2B) and their corresponding co-crystal structures with BpMip; PDB ID 5V8T for **2** and PDB ID 4G50 for **3**. The part of the molecule that was subsequently chosen as position for linker attachment is marked in pink in the chemical structure. As can be seen from the crystal structures, in each case, the pipecoline ring is located deep in the active site pocket and the phenyl ring of the sulfonamide moiety occupies a sub-pocket, whereas the ether-substituted benzene moiety (for **2**) and the trimethoxyphenyl moiety (for **3**) are located on the protein surface. This part of the molecule constitutes a suitable area for the attachment of the linker without affecting binding to Mip. Non-carbon atoms are colored as follows: red, oxygen; blue, nitrogen; yellow, sulfur.

The suitability for medium or upscaling to high throughput screening (HTS) is reflected by the Z-factor [41]: $= 1 - \frac{(3\sigma^+ + 3\sigma^-)}{|\mu^+ - \mu^-|}$, where the mean values and standard deviations for the negative and positive controls are indicated by μ^-, σ^- and μ^+, σ^+, respectively. The triplicate investigation of 12 samples each resulted in a Z-factor of 0.89 (Supplementary information). This result of well over 0.5 even guarantees suitability for HTS.

Competitive displacement assay for the screening of BpMip inhibitors

Based on their broad range of K_i values in the previously used PPIase assay, six inhibitors were selected to be tested in the developed competitive displacement FP assay (Table 1). In the following, using the probe **1**, it was possible to distinguish between moderately strong inhibitors, such as **11** (SF235, see Table 1), and strong inhibitors, such as **12** (Fig. 6; SF339, Table 1). The trends from the previously used kinetic enzyme assay are congruent with the results obtained in the FP assay (Table 1 and Supplementary data). Minor differences can be explained by the fact that the FP assay measures affinity to the binding pocket, whereas the enzyme assay measures the effect on enzyme activity. In addition, the assays are performed at different temperatures.

The determined K_D of **8** was 2.36 ± 0.27 μM, which is close to that of probe **1**. Since **8** corresponds to the inhibitor moiety of probe **1** except for the Cbz protecting group, it can be concluded that fluorescein labeling in probe **1** has no significant effect on protein binding. Using the established FP competition assay, we were able to screen out enzymatically ineffective inhibitors such as the racemic compound **13** (K_D = 10.64 μM, see Table 1).

Conclusion

In this study, an FPA has been established to enable the screening and effective development of BpMip inhibitors. A fluorescent probe derived from previous pipecolic scaffold Mip inhibitors was labeled with fluorescein. This probe showed moderate affinity for the PPIase domain of the BpMip protein and enabled a highly robust FPA suitable for screening large compound libraries with medium to high throughput (Z ~ 0.89) to identify potent new inhibitors. A moderate K_D of 2.0 μM renders **1** a useful tracer for moderate BpMip inhibitors and a good complement to the previously reported FKBP and Mip tracers. [25,26]

The developed FPA has several advantages: it is very fast to perform, robust, can be easily parallelized, and the data processing is straightforward. Unlike SPR, this assay shows that the small molecule binds at the protein site of interest through competitive binding. The assay is suitable for both HTS and detailed hit analysis. Any new small molecule can be tested without derivatization or isotopic labeling. Limitations include that binding affinity does not provide concrete information on enzymatic activity, and that the assay's detection limit of ~200-400 nM may be insufficient for some applications.

The results obtained with the FPA are in line with the findings of the frequently used protease-coupled PPIase assay. Analysis of the tempera-

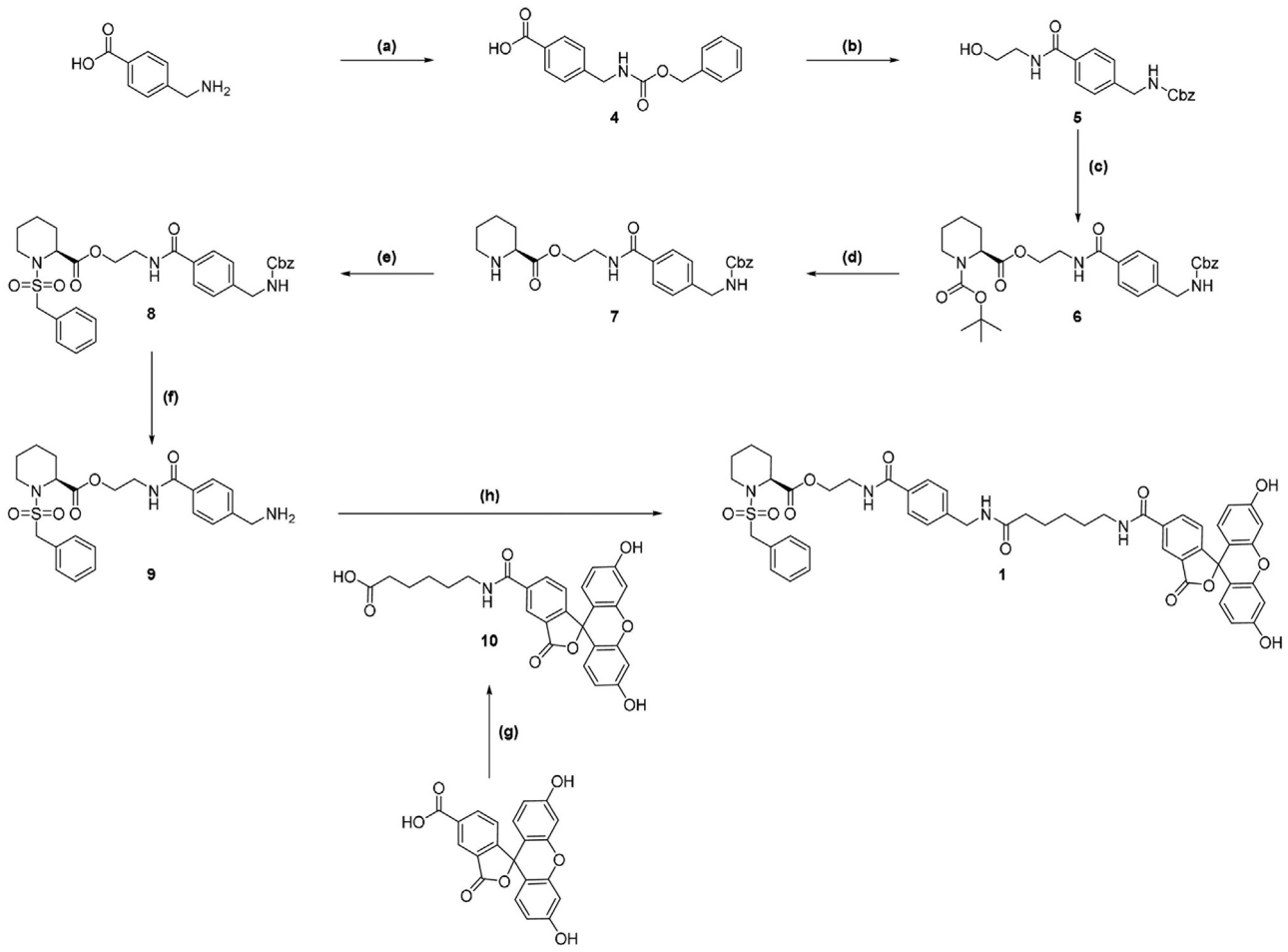

Fig. 3. Synthesis pathway of the fluorescent probe **1** and the intermediate product **8**. Reagents and conditions: (a) CBz-Cl, $NaHCO_3$, water/THF (1:1), 1 d, rt, 99%; (b) ethanolamine, EDC-HCl, HOBt, DCM, rt, 1 d, 87%; (c) (*S*)-*N*-Boc-pipecolic acid, DCC, DMAP, DCM/DMF (3:1), rt, 4 h, 48%; (d) TFA, DCM, rt, 2.5 h, 93%; (e) NEt_3, DCM, phenylmethanesulfonyl chloride, rt, 3 d, 44%; (f) Pd/C (10 wt%), H_2 (10 bar), acetic acid, MeOH, rt, 2 d, 13%; (g) i) HBTU, 6-methoxy-6-oxohexane-1-aminium chloride, NEt_3, DMF, rt, 18 h, ii) LiOH, water, rt, 1 d, 33%; (h) HBTU, DIPEA, fluorescein-5-hexanoic acid, DCM/DMF (2:1), rt, 1 d, 44%.

ture dependence of the probe's binding highlighted that BpMip's ligand binding is driven by enthalpic rather than entropic effects.

The assay presented here may contribute to the development of novel therapeutics against melioidosis and other microbial diseases.

Methods

Chemicals. Reagents used for the synthesis in this work were obtained from *Alfa Aesar* (Ward Hill, USA), *Merck* (Darmstadt, Germany), *Avantor* (Darmstadt, Germany), *TCI Deutschland GmbH* (Eschborn, Germany), *Fisher Scientific* (Schwerte, Germany), and *ABCR* (Karlsruhe, Germany). The purchased chemicals were used without further purification. Dry solvents for organic synthesis were produced and stored according to general procedures [42].

Gravity-driven column chromatography. For gravity-driven column chromatography, silica gel 60 (0.063 – 0.200 nm) purchased from *Merck* (Darmstadt, Germany) was used.

Flash chromatography. For purification by medium pressure liquid chromatography (MPLC, flash chromatography), a *puriFlash®430* system from Interchim (Montluçon, France) with an integrated UV diode array detector (DAD) with a scanning range of 200 – 600 nm was used. Non-UV-active compounds were detected using a *Flash-ELSD* (evaporative light scattering detector) version 2011 from *Interchim* (Montluçon, France). The following pre-packed columns were used: *Chromabond Flash*, type: RS15 C18 ec, 16 g from *Macherey-Nagel* (Düren, Germany) and *puriFlash*, type: SI-Std (IR-50SI), 12 g and 25 g from *Interchim* (Montluçon, France).

HPLC. Purity analysis was carried out using an HPLC (high performance liquid chromatography) system from *Shimadzu Scientific instruments* (Kyoto, Japan). Mobile phase A was Milli-Q®-water with 0.1% formic acid (FA) added, while mobile phase B was MeOH with 0.1% FA. The gradient started with 5% of mobile phase B and the ratio of mobile phase B was increased to 100% over 8 min and held for 4 min. For re-equilibration, the mobile phase B ratio was reduced from 100% to 5% in another 4 min. Subsequently, the column was flushed with 5% B for 2 min. The flow rate was set to 1.0 mL/min. The injection volume was 20 µL. The UV signal at 254 nm was chosen for detection, with the oven set to room temperature.

TLC. Thin layer chromatography (TLC) was performed on pre-coated silica gel glass plates SIL G-25 (*Macherey-Nagel*, Düren, Germany). Spots were evidenced by quenching at 254 nm or intrinsic fluorescence at 365 nm.

High-Resolution Mass Spectrometry (HRMS) was performed using an *Agilent* Infinity II LC-system (Waldbronn, Germany) consisting of a quaternary pump, a thermostatted autosampler and a thermostatted column compartment, coupled to a *Sciex* X500R QTOF mass spectrometer (Concord, Ontario, Canada) equipped with a Turbo V™ Ion Source (ESI). Automatic calibration of the mass spectrometer was performed using the provided tuning solution for ESI (*Sciex*, Concord, Ontario, Canada). Mobile phase A was a mixture of water and 0.1% FA,

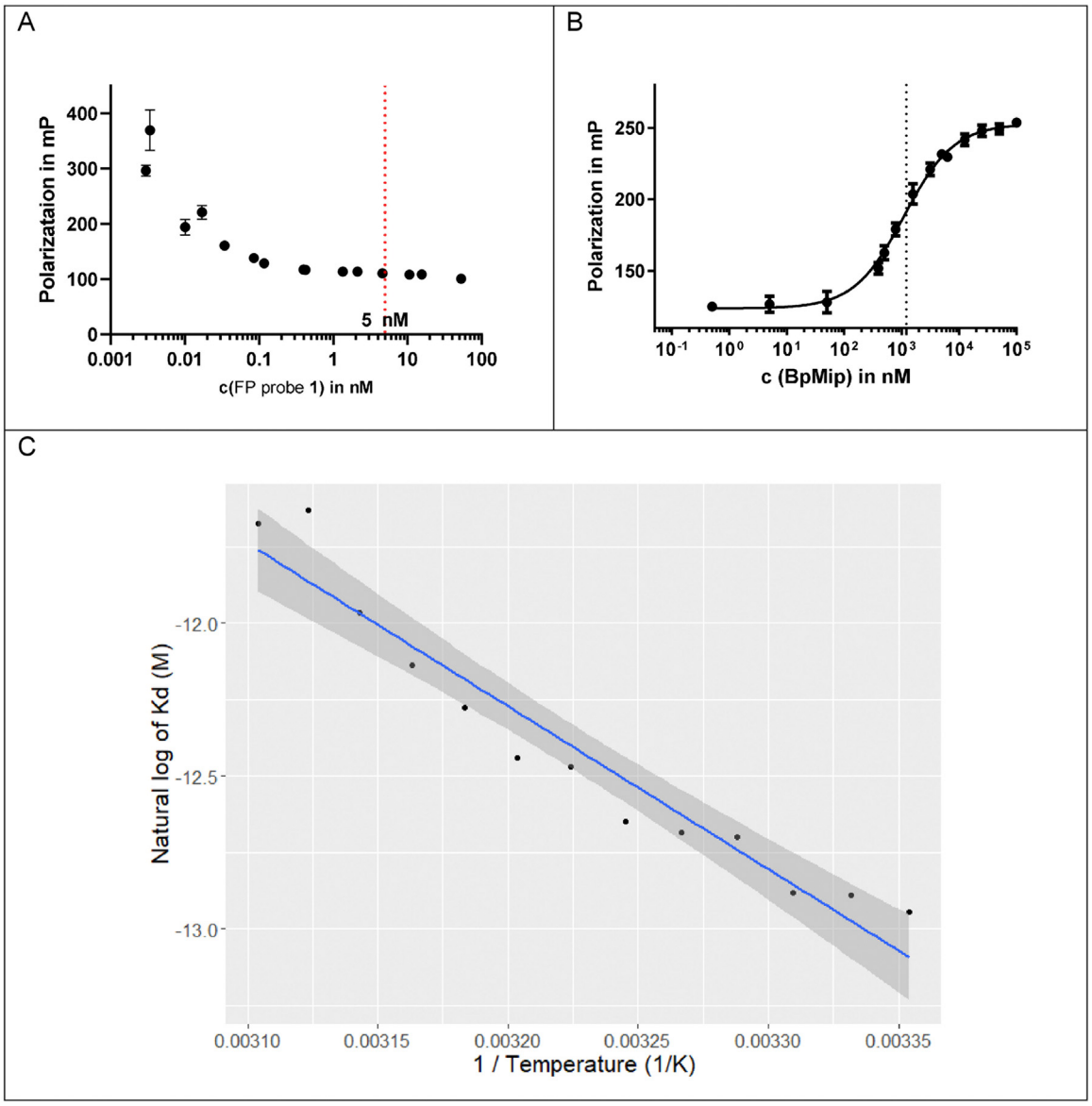

Fig. 4. A: Stable, concentration-independent polarization was demonstrated in a sensitivity test by measuring a dilution series of the tracer molecule **1** for a range from 0.5 nM to 50 nM. B: An exemplary FP equilibrium saturation binding curve of BpMip and probe **1** at a concentration of 5 nM at 25°C. Error bars represent standard error, with data points showing the mean of three scans of each well. A triple repetition resulted in a K_D of 1200 ± 120 nM (dashed line). Triplicate is shown in the SI. C: Affinity was tested across a range of temperatures from 25°C to 55°C. The interaction showed a linear van't Hoff plot, suggesting that the heat capacity of the protein is unaffected by temperature. Thus, the enthalpy (ΔH°) and entropy (ΔS°) were determined to be -44 ± 3 kJ mol^{-1} and -39 ± 11 J mol^{-1}, respectively. Upper images were generated using GraphPad Prism v8.0.1; Fig. 4C was generated using *R* v. 4.2.1.

while mobile phase B was acetonitrile with 0.1% FA. An isocratic elution of 50% B with a stop time of 1.5 min was used. The flow rate was set to 1 mL/min and the injection volume was 10 μL. The parameters for the HRMS experiment were optimized by flow-injection using positive polarity (Gas1: 50 psi, Gas2: 50 psi, Curtain gas: 25 psi, Ionspray voltage: 5500 V, Temperature: 500°C, Declustering potential: 70 +/- 10 V, Collision energy: 10 V).

Infrared Spectroscopy (IR). IR spectra were recorded on a Jasco-FT-IR-6100 system (*Jasco Deutschland GmbH*, Groß-Umstadt, Germany) in combination with a diamond ATR accessory. The wave numbers of characteristic absorption bands are given in [cm^{-1}] and categorized according to their strength (vs = very strong, s = strong, m = medium, w = weak, br = broad).

Nuclear magnetic resonance spectroscopy. ^{1}H (400.132 MHz) and ^{13}C (100.613 MHz) NMR spectra were recorded on a Bruker AV 400 instrument (*Bruker Biospin*, Ettlingen, Germany) at a temperature of 300 K. The signal of the respective deuterated solvent was used as internal standard ($CDCl_3$: ^{1}H: 7.26 ppm, ^{13}C: 77.16 ppm; CD_3OD: ^{1}H: 3.31 ppm, ^{13}C: 49.00 ppm; DMSO-d^{6}: ^{1}H: 2.50 ppm, ^{13}C: 39.52 ppm) [43]. Abbreviations for multiplicity are: s, singlet; d, doublet; t, triplet; m, multiplet; br, broad; dd, doublet of doublets; ddd, doublet of doublets of doublets. MestReNova® (version 6.0.2-5475) software (*Mestrelab Research S.L.*, Santiago de Compostela, Spain) was applied for processing of NMR spectra.

Melting points. To determine melting points, an MP70 melting point system (*Mettler-Toledo GmbH*, Gießen, Germany) was used. The results are not corrected.

Synthesis of the investigated Mip inhibitors. The selected inhibitors **11, 15, 14**, and **2** and the corresponding synthesis have been described by Seufert et al. [18] **13** was synthesized using precursor 3-(pyridin-3-yl)propyl (*R, S*)-1-((4-aminobenzyl)sulfonyl) piperidine-2-carboxylate, described in the same publication. The synthesis of **12** has

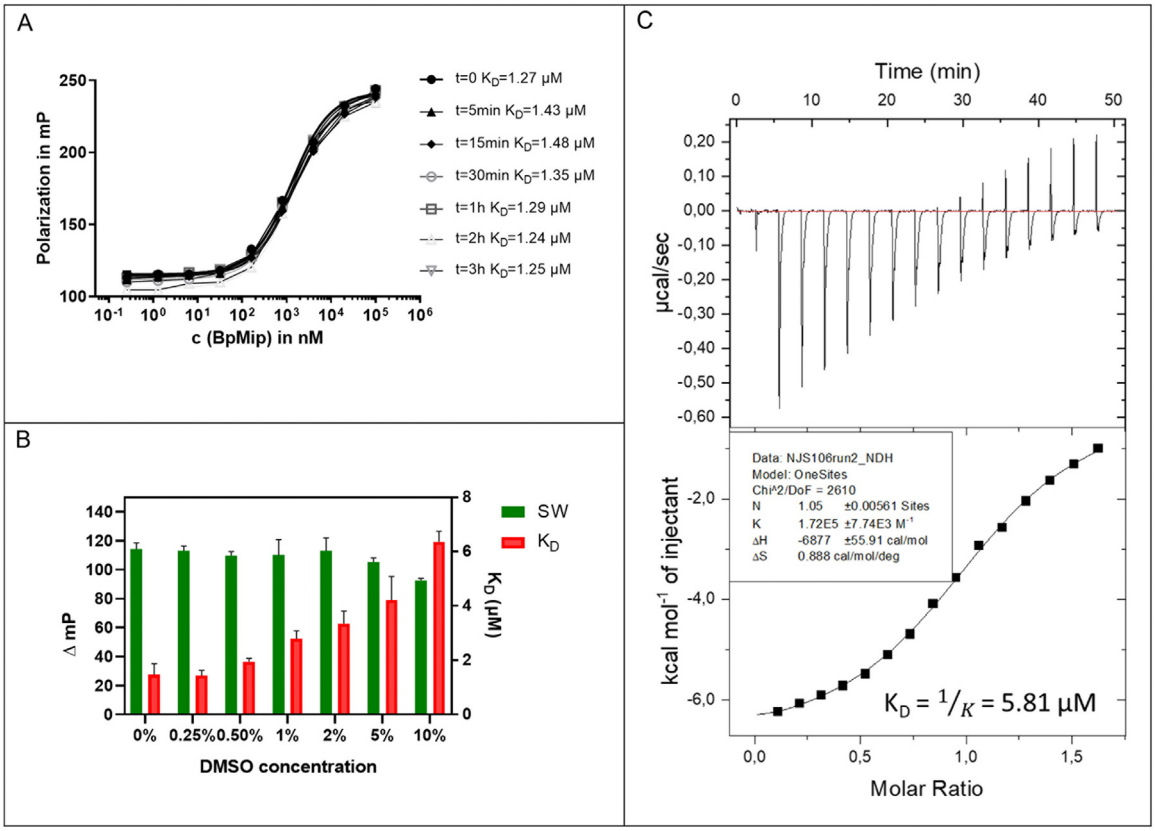

Fig. 5. Validation of the FP experiment. A: Time-dependent equilibrium study. Fluorescence polarization was measured at timepoints from 5 minutes to three hours after experiment setup. The results are within error of each other, indicating that the enzyme-substrate complex is formed in the first few minutes after setup and was stable for at least three hours. B: In a DMSO tolerance assay, an active site titration was performed in the presence of a defined DMSO concentration and the change in binding capacity of the tracer was determined using the K_D value and the signal window (SW), calculated from a duplicate at least. For higher DMSO concentrations, the MSR of the K_D values relative to 0 % DMSO was calculated (SI). If the common criterion of an MSR of less than 3 is used, a significant deviation is obtained at 10 % DMSO. GraphPad Prism 8.0.1 was used for calculation and graphical representation. C: The binding affinity of probe **1** was verified using isothermal titration calorimetry. Three independent experiments were performed, injecting probe **1** into a solution of BpMip. An exemplary ITC plot is shown, giving a stoichiometric ratio of $N = 1.05 \pm 0.006$ and a K_D of 5.81 ± 0.26 µM at 3 % DMSO.

been described by Iwasaki et al. [3] **8** is an intermediate of tracer **1** synthesis and is described there. All compounds used had a purity >95% according to HPLC. Purity data are shown in the SI.

Synthesis of 3-(Pyridin-3-yl)propyl (*R/S*)-1-((4-acetamidobenzyl)sulfonyl)piperidine-2-carboxylate (13). Following a modified procedure by Baer et al., [44] to a solution of 3-(pyridin-3-yl)propyl (*R, S*)-1-((4-aminobenzyl)sulfonyl)piperidine-2-carboxylate (100 mg, 240 µmol) in dry DCM (20 mL) were added acetic anhydride (23 µL, 240 µmol) and NEt_3 (66 µL, 479 µmol) under ice cooling. After completion of the reaction monitored by TLC (SiO_2, petroleum ether (PE)/EA 1:10), the reaction mixture was loaded directly onto silica gel and purified by flash chromatography (SiO_2, A: PE, B: EA, gradient: 50% → 100% B). **13** was obtained as a yellowish oil in a yield of 91% (100 mg, 281 µmol). $R_f = 0.10$ (SiO_2, PE/EA 1:10), IR (ATR, $\tilde{\upsilon}_{max}$ [cm^{-1}]): 3308 (w), 3038 (w), 2940 (w), 2859 (w), 1733 (m), 1672 (m), 1534 (m), 1513 (m), 1371 (m), 1325 (m), 1176 (m), 1127 (s), 843 (m). ^{1}H NMR ($CDCl_3$): δ = 8.50 – 8.42 (m, 2H), 7.69 (s, 1H), 7.56 – 7.47 (m, 3H), 7.42 – 7.33 (m, 2H), 7.25 – 7.20 (m, 1H), 4.50 (d, 1H, ^3J = 4.6 Hz), 4.25 – 4.10 (m, 4H), 3.49 – 3.42 (m, 1H), 3.17 (ddd, 1H, ^2J = 12.8 Hz, ^3J = 12.8, 2.9 Hz), 2.72 (t, 2H, ^3J = 7.8 Hz), 2.17 – 2.07 (m, 4H), 2.03 – 1.93 (m, 2H), 1.73 – 1.55 (m, 3H), 1.50 – 1.35 (m, 1H), 1.29 – 1.12 (m, 1H) ppm. ^{13}C NMR ($CDCl_3$): δ = 171.4, 168.7, 149.7, 147.5, 138.7, 136.3, 136.0, 131.4 (2C), 124.4, 123.5, 119.6 (2C), 64.2, 58.3, 56.0, 43.4, 29.8, 29.1, 27.8, 24.9, 24.4, 20.3 ppm. Purity (HPLC): 99.4%. HRMS (m/z) $C_{23}H_{29}N_3O_5S$, $(M+H)^+$, calculated 460.19007, found 460.18955, error: 1.1 ppm.

Synthesis of tracer 1

Synthesis of 4-((((Benzyloxy)carbonyl)amino)methyl)benzoic acid (4). 4 was synthesized according to a protocol by Lameijer et al., [45] using 11.0 g of 4-aminomethylbenzoic acid (72.8 mmol), sodium hydrogen carbonate (7.34 g, 87.3 mmol) and benzyl chloroformate (12.4 mL, 87.3 mmol) in a mixture of THF and water (1:1; 200 mL). **4** was obtained quantitatively as a white powder (20.8 g, 72.8 mmol, > 99%; Lit.: [45] 83%). R_f = 0.46 (DCM/MeOH 9:1), IR (ATR, $\tilde{\upsilon}_{max}$ [cm^{-1}]): 3340 (s), 3062 (w), 3034 (w), 2927 (m), 1683 (s), 1602 (s), 1550 (s), 1529 (s), 855 (w), 803 (w), 774 (m), mp: 320°C under decomposition. ^{1}H NMR (CD_3OD): δ = 7.95 – 7.87 (m, 2H), 7.39 – 7.15 (m, 7H), 5.11 (s, 2H), 4.34 (s, 2H) ppm. ^{13}C NMR (CD_3OD): δ = 173.8, 159.1, 143.6, 138.0, 135.5, 130.5 (2C), 129.4 (2C), 129.0, 128.7 (2C), 127.7 (2C), 67.6, 45.2 ppm. The recorded spectra are in agreement with the literature [45].

Synthesis of Benzyl (4-((2-hydroxyethyl)carbamoyl)benzyl)carbamate (5). To a solution of **4** (7000 mg, 24.5 mmol) in dry DCM (150 mL), HOBt (3315 mg, 24.5 mmol) and EDC · HCl (4703 mg, 24.5 mmol) were added under ice cooling and allowed to stir for 15 min. Subsequently, 2-aminoethan-1-ol (2.35 mL, 39.2 mmol) was added to the solution under ice cooling. The reaction was allowed to warm to rt and stirred for 2 d, monitored by TLC (SiO_2, DCM/MeOH 10:1). The solvent was removed under reduced pressure, the crude oily product was loaded directly onto silica gel and purified by flash chromatography (SiO_2, A: DCM, B: MeOH, gradient: 0 → 25% B). **5** was obtained as

Table 1
Chemical structures of the Mip inhibitors examined and their respective K_i values determined by the established FP assay compared with the protease-coupled PPIase assay [20]. More detail is provided in supplementary information.

Inhibitor	Structure	K_i [μM], *FP*	K_i [μM], *PPIase*
11	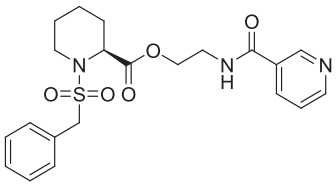	1.79 ± 0.33	0.29 ± 0.06
2	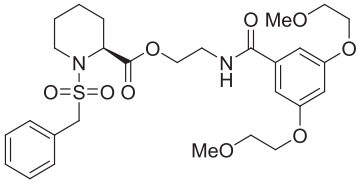	1.15 ± 0.74	0.98 ± 0.29
12	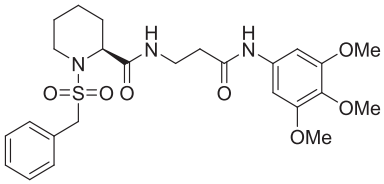	0.46 ± 0.01	0.45 ± 0.09
14	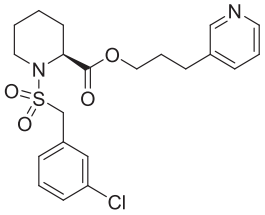	0.65 ± 0.08	0.18 ± 0.01
13	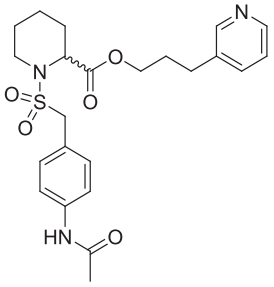	10.64 ± 0.53	21.0 ± 8.0
15	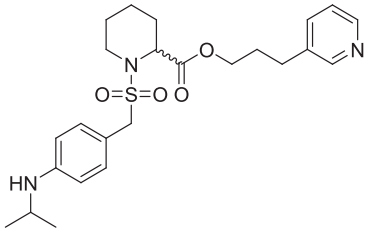	15.10 ± 5.10	4.50 ± 1.70
8	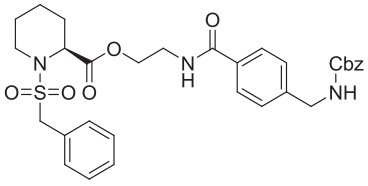	2.36 ± 0.27	*Not determined*

a white solid in a yield of 87% (7.00 g, 21.3 mmol). R_f = 0.47 (SiO_2, DCM/MeOH 10:1), mp: 165°C, IR (ATR, $\tilde{\upsilon}_{max}$ [cm^{-1}]): 3383 (s), 3142 (s) 2922 (s), 1692 (s), 1656 (s), 1592 (s), 1270 (s), 834 (s), 776 (s), 710 (s). ^{1}H NMR (DMSO-d_6): δ = 8.36 (t, ^3J = 5.6 Hz, 1H), 7.86 (t, ^3J = 6.1 Hz, 1H), 7.83 – 7.75 (m, 2H), 7.41 – 7.28 (m, 7H), 5.05 (br s, 2H), 4.70 (t, ^3J = 5.6 Hz, 1H), 4.25 (d, ^3J = 6.1 Hz, 2H), 3.50 (dt, ^3J = 6.1, 5.9 Hz, 1H), 3.35 – 3.29 (m, 2H) ppm. ^{13}C NMR (DMSO-d_6): δ = 166.1, 156.4, 142.8, 137.1, 133.1, 128.4 (2C), 127.8, 127.7, 127.2 (2C), 126.7 (2C), 65.4, 59.8, 43.6, 42.1 ppm.

Synthesis of 2-(2-(4-((((Benzyloxy)carbonyl)amino)methyl)benzamido)ethyl)-1-(*tert*-butyl-*S*)-piperidine-1,2-dicarboxylate (6). To

a solution of (*S*)-1-(*tert*-butoxycarbonyl)piperidine-2-carboxylic acid (5.00 g, 21.8 mmol) in a mixture of dry DCM (150 mL) and dry DMF (50 mL), catalytic amounts of DMAP (500 mg, 4.09 mmol) and an excess of EDC · HCl (3.00 g, 15.7 mmol) were added under ice cooling and allowed to stir for 15 min. **5** (4.30 g, 13.1 mmol) was added to the solution under ice cooling, the reaction was allowed to warm to rt and stirred for 1 d, monitored by TLC (SiO_2, DCM/MeOH 20:1). The solvent was removed *in vacuo*, the residue suspended in DCM and the mixture filtered. The solvent of the filtrate was removed *in vacuo*. The crude oily product was loaded directly onto silica gel and purified by column chromatography (SiO_2, PE/EA 1:1, followed by PE/EA/MeOH 1:0.9:0.1). After subsequent purification by flash chromatography (SiO_2, A: PE, B: EA, gradient: 0 → 50% B, ELSD), **6** was obtained as a colorless oily solid in a yield of 48% (3400 mg, 6.30 mmol). R_f = 0.17 (SiO_2, DCM/MeOH 20:1), IR (ATR, $\tilde{\upsilon}_{max}$ [cm^{-1}]): 3321 (m), 2932 (m), 1694 (s), 1643 (s), 1535 (s), 1245 (s), 1155 (s) 870 (w), 753 (w), 738 (w). ^{1}H NMR ($CDCl_3$): δ = 7.84 – 7.74 (m, 2H), 7.40 – 7.28 (m, 7H), 5.18 – 5.09 (m, 3H), 4.78 (br s, 1H), 4.50 – 4.20 (m, 4H), 4.02 – 3.52 (m, 3H), 3.06 – 2.70 (m, 2H), 2.24 – 2.14 (m, 1H), 1.76 – 1.55 (m, 4H), 1.41 (br s, 9H), 1.31 – 1.11 (m, 1H) ppm. ^{13}C NMR ($CDCl_3$): δ = 172.5, 167.1, 156.7, 156.6, 142.5 (br s, 1C), 136.5, 133.4, 128.7 (br s, 2C), 128.4 (br s, 1C), 128.3 (br s, 2C), 127.64 (br s, 2C), 127.59 (br s, 2C), 80.4, 67.2, 64.0, 54.5 (br s, 1C), 44.9, 42.7 & 39.3 (br s, 1C, *rotamers*), 38.8, 28.5 (s, 3C), 26.6, 24.7, 20.8 ppm.

Synthesis of 2-(4-((((Benzyloxy)carbonyl)amino)methyl)benzamido)ethyl (*S*)-piperidine-2-carboxylate (7). To a solution of **6** (2700 mg, 5.00 mmol) in dry DCM (25 mL) was slowly added 5.00 mL of TFA (65.0 mmol) at rt and the mixture was stirred for 2.5 h, monitored by TLC (SiO_2, DCM/MeOH 20:0.5). Subsequently, the reaction mixture was washed with aqueous saturated $NaHCO_3$ solution (3 · 20 mL) and with water (3 · 20 mL). The phases were separated, the organic phase was dried over sodium sulphate and filtrated. After removal of the organic solvent *in vacuo*, **7** was obtained as a white oily solid in a yield of 93% (2043 mg, 4.65 mmol). R_f = 0.23 (SiO_2, DCM/MeOH 20:0.5), IR (ATR, $\tilde{\upsilon}_{max}$ [cm^{-1}]): 3331 (s), 3033 (w), 2930 (m), 1738 (w), 1686 (s), 1636 (s), 1534 (s), 1202 (m), 848 (w), 746 (w). ^{1}H NMR ($CDCl_3$): δ = 7.74 – 7.68 (m, 2H), 7.39 – 7.27 (m, 7H), 6.79 (br s, 1H), 5.34 (br s, 1H), 5.13 (s, 2H), 4.40 (br d, ^3J = 5.9 Hz, 2H), 4.32 (t, ^3J = 5.2 Hz, 2H), 3.74 – 3.67 (m, 2H), 3.38 (dd, ^3J = 9.9, 3.1 Hz, 1H), 3.10 – 3.03 (m, 1H), 2.68 – 2.60 (m, 1H), 2.29 (br s, 1H), 1.99 – 1.92 (m, 1H), 1.81 – 1.74 (m, 1H), 1.60 – 1.40 (m, 4H) ppm. ^{13}C NMR ($CDCl_3$): δ = 174.0, 167.4, 156.6, 142.4 (br s, 1C), 136.5, 133.4, 128.7 (br s, 2C), 128.33 (br s, 1C), 128.27 (br s, 2C), 127.6 (br s, 2C), 127.5 (br s, 2C), 67.1, 63.8, 58.8 (br s, 1C), 45.8, 44.8, 39.6, 29.4, 25.8, 24.1 ppm.

Synthesis of 2-(4-((((Benzyloxy)carbonyl)amino)methyl)benzamido)ethyl (*S*)-1-(benzylsulfonyl)piperidine-2-carboxylate (8). To a solution of **7** (2350 mg, 5.35 mmol) in dry DCM (50 mL), NEt_3 (1.94 mL, 13.9 mmol) and phenylmethanesulfonyl chloride (1175 mg, 6.04 mmol) were added under ice cooling. The solution was immediately allowed to warm to rt and stirred for 3 d, monitored by TLC (SiO_2, PE/EA 1:3). Subsequently, the mixture was washed with diluted acetic acid (0.1 M, 50 mL) and saturated ammonium chloride solution (30 mL). The phases were separated, the organic solvent was removed *in vacuo,* and the crude oily product was purified by flash chromatography (Run 1: SiO_2, A: DCM, B: MeOH, gradient: 0% → 30% B; Run 2: SiO_2, A: CyH, B: EA, gradient: 0% → 100% B). **8** was obtained as white oily solid in a yield of 44% (1400 mg, 2.36 mmol). R_f = 0.68 (SiO_2, PE/EA 1:3), IR (ATR, $\tilde{\upsilon}_{max}$ [cm^{-1}]): 3346 (br m), 2946 (m), 1704 (s), 1644 (s), 1534 (s), 1505 (s), 1321 (s), 847 (w), 824 (w), 781 (w). ^{1}H NMR ($CDCl_3$): δ = 7.84 – 7.79 (m, 2H), 7.42 – 7.28 (m, 12H), 7.13 (t, ^3J = 5.4 Hz, 1H), 5.19 – 5.11 (m, 3H), 4.49 – 4.41 (m, 3H), 4.27 – 4.16 (m, 4H), 3.83 – 3.68 (m, 2H), 3.33 (d, ^2J = 12.8 Hz, 1H), 3.08 (ddd, ^2J = 12.8, ^3J = 12.8, 2.7 Hz, 1H), 2.13 (br d, ^2J = 13.4 Hz, 1H), 1.70 – 1.54 (m, 2H), 1.48 – 1.28 (m, 2H), 1.19 – 1.08 (m, 1H) ppm. ^{13}C NMR ($CDCl_3$): δ = 171.4, 167.2, 156.6, 142.1, 136.5, 133.3, 131.0 (2C), 129.2, 129.0, 128.8 (2C), 128.7 (2C), 128.4, 128.3 (2C), 127.8 (2C), 127.5 (2C), 67.1, 64.9, 59.2, 56.7, 44.9, 44.2, 38.9, 27.2, 24.8, 20.2 ppm. Purity (HPLC): 95.1%. HRMS (m/z) $C_{31}H_{35}N_3O_7S$, $(M+H)^+$, calculated 594.22685, found 594.22775, error: 1.5 ppm.

Synthesis of 2-(4-(Aminomethyl)benzamido)ethyl (*S*)-1-(benzylsulfonyl)piperidine-2-carboxylate (9). To a solution of **8** (450 mg, 758 µmol) in methanol (15 mL) and acetic acid (1 mL, 1 mol/L), catalytic amounts of palladium on charcoal (10 wt-%, 84 mg, 79 µmol) were added at rt under an Argon atmosphere. The reaction mixture was then stirred for 1 d at rt under a hydrogen pressure of 10 bar. Subsequently, the catalyst was removed over celite, which was then extracted with methanol (50 mL). The solvent was removed *in vacuo*. The residue was diluted with DCM (50 mL) and washed with saturated sodium hydrogen carbonate solution (2 · 20 mL). After separation of the phases, the solvent of the organic phase was removed *in vacuo,* and the crude oily product was purified by flash chromatography (SiO_2, A: DCM, B: MeOH, gradient: 0% → 20% B). **9** was obtained as a slightly yellowish solid in a yield of 13% (45 mg, 99 µmol). R_f = 0.11 (SiO_2, DCM/MeOH 9:1), mp: 85°C, IR (ATR, $\tilde{\upsilon}_{max}$ [cm^{-1}]): 3310 (br m), 2932 (m), 2857 (m), 1733 (s), 1637 (s), 1539 (s), 1498 (s), 1320 (s), 845 (w), 782 (w). ^{1}H NMR ($CDCl_3$, protonated form of **9**): δ = 7.85 – 7.80 (m, 2H), 7.44 – 7.34 (m, 7H), 7.16 (t, ^3J = 5.7 Hz, 1H), 4.47 – 4.40 (m, 1H), 4.30 – 4.19 (m, 4H), 3.93 (br s, 2H), 3.83 – 3.70 (m, 2H), 3.33 (br d, ^2J = 12.7 Hz, 1H), 3.08 (ddd, ^2J = 12.7, ^3J = 12.7, 2.7 Hz, 1H), 2.26 (br s, 3 H), 2.12 (br d, ^2J = 13.3 Hz, 1H), 1.65 – 1.55 (m, 2H), 1.50 – 1.10 (m, 3H) ppm. ^{13}C NMR ($CDCl_3$, protonated form of **9**): δ = 171.5, 167.4, 145.7, 132.9, 131.0 (2C), 129.2, 128.9, 128.8 (2C), 127.7 (2C), 127.4 (2C), 64.9, 59.2, 56.7, 46.0, 44.1, 38.9, 27.3, 24.8, 20.2 ppm.

Synthesis of 6-(3′,6′-Dihydroxy-3-oxo-3*H*-spiro[isobenzofuran-1,9′-xanthene]-5-carboxamido)hexanoic acid (10). To a mixture of 5-carboxyfluorescein (495 mg, 1.25 mmol), 6-methoxy-6-oxohexane-1-aminium chloride (204 mg, 1.12 mmol), and NEt_3 (0.36 mL, 2.62 mmol) in dry DMF (20 mL), HBTU (507 mg, 1.34 mmol) was added at rt and stirred overnight. After removal of DMF *in vacuo*, the crude oily product obtained was treated with a solution of lithium hydroxide (0.4 M, 31.2 mL, 12.5 mmol) at rt for 1 d. The pH was then adjusted to 5 with diluted hydrochloric acid (10 mL, 1 M) under ice cooling. The solvent was removed *in vacuo*, the mixture was directly loaded onto silica gel, and the crude oily product was purified by flash chromatography (SiO_2, A: DCM + 0.5% FA, B: MeOH + 0.5% FA, gradient: 0% → 10% B). **10** was obtained as an orange solid in a yield of 33% (180 mg, 368 µmol). R_f = 0.28 (SiO_2, $CHCl_3$/MeOH 9:1 + 1% FA; 365 nm), mp: 262°C (under decomposition), IR (ATR, $\tilde{\upsilon}_{max}$ [cm^{-1}]): 3043 (m), 2936 (m), 1707 (m), 1666 (m), 1577 (vs), 1530 (vs), 1455 (vs), 1295 (vs), 850 (m), 760 (m). ^{1}H NMR (CD_3OD): δ = 8.41 (br s, 1H), 8.19 (dd, ^3J = 8.0, ^4J = 1.5 Hz, 1H), 7.29 (d, ^3J = 8.0 Hz, 1H), 6.69 (d, ^4J = 2.3 Hz, 2H), 6.59 (d, ^3J = 8.7 Hz, 2H), 6.53 (dd, ^3J = 8.7, ^4J = 2.3 Hz, 2H), 3.44 (t, ^3J = 7.2 Hz, 2H), 2.33 (t, ^3J = 7.2 Hz, 2H), 1.74 – 1.63 (m, 4H), 1.51 – 1.41 (m, 2H) ppm. ^{13}C NMR (CD_3OD): δ = 177.5, 170.6, 168.4, 161.4 (br s, 2C), 156.6, 154.0 (2C), 138.1, 135.5, 130.1 (2C), 128.7, 125.7, 124.7, 113.7 (2C), 110.9 (2C), 103.6 (2C), 82.3, 41.1, 34.8, 30.1, 27.6, 25.8 ppm. The molecule is known in the literature, [46] but no synthesis or analytical data have been reported to date.

Synthesis of 2-(4-((6-(3′,6′-Dihydroxy-3-oxo-3H-spiro[isobenzofuran-1,9′-xanthene]-5-carboxamido)hexanamido)methyl)benzamido)ethyl (*S*)-1-(benzylsulfonyl)piperidine-2-carboxylate (1). To a solution of **10** (32 mg, 65 µmol) in a mixture of dry DCM (10 mL) and DMF (5 mL), HBTU (33 mg, 88 µmol) and DIPEA (100 µL, 570 µmol) were added under ice cooling and allowed to stir for 15 min. Subsequently, compound **9** (30 mg, 65 µmol) was added to the solution under ice cooling, the reaction was allowed to warm to rt and stirred for 1 d, monitored by TLC (SiO_2, DCM/MeOH 10:1 + 1% FA). Saturated ammonium chloride solution (10 mL) was added, the solvent was removed *in vacuo*, and the crude oily product was directly loaded onto silica gel. After purification by flash chromatography (Run 1: SiO_2, A: DCM,

B: MeOH, gradient: 0 → 20% B; Run 2: RP 18, A: H_2O + 0.1% FA, B: ACN + 0.1% FA, gradient: 5% → 40% B), **1** was obtained as a yellow solid in a yield of 44% (27 mg, 29 µmol). R_f = 0.40 (SiO_2, DCM/MeOH 10:1 + 1% FA, 365 nm), mp: 160°C, IR (ATR, $\tilde{\upsilon}_{max}$ [cm^{-1}]): 3341 (br, s), 3080 (br, s), 2941 (s), 1740 (s), 1704 (s), 1636 (vs), 1613 (vs), 1319 (s), 1109 (vs), 847 (m), 740 (m). ^{1}H NMR (CD_3OD): δ = 8.42 (br s, 1H), 8.17 (dd, ^3J = 8.0, ^4J = 1.5 Hz, 1H), 7.79 – 7.75 (m, 2H), 7.42 – 7.37 (m, 2H), 7.36 – 7.31 (m, 5H), 7.28 (d, ^3J = 8.0 Hz, 1H), 6.69 (d, ^4J = 2.3 Hz, 2H), 6.60 (d, ^3J = 8.7 Hz, 2H), 6.53 (dd, ^3J = 8.7, ^4J = 2.3 Hz, 2H), 4.44 – 4.38 (m, 3H), 4.38 – 4.33 (m, 2H), 4.33 – 4.30 (m, 2H), 3.73 – 3.61 (m, 2H), 3.46 – 3.36 (m, 3H), 3.14 (ddd, ^2J = 12.8, ^3J = 12.8, 2.8 Hz, 1H), 2.30 (t, ^3J = 7.3 Hz, 2H), 2.14 – 2.07 (m, 1H),1.77 – 1.64 (m, 4H), 1.60 – 1.32 (m, 6H), 1.24 – 1.15 (m, 1H) ppm. ^{13}C NMR (CD_3OD): δ = 176.1, 172.8, 170.6, 170.0, 168.4, 161.3 (2C), 154.3 (2C), 144.3, 138.0, 135.2, 134.2, 132.2 (2C), 131.0, 130.3 (2C), 129.50–129.45 (m, 3C), 128.65–128.57 (m, 6C), 125.9, 125.0, 114.0 (2C), 111.1 (2C), 103.6 (2C), 82.0, 64.8, 59.4, 57.3, 44.6, 43.7, 41.0, 40.0, 36.9, 30.1, 28.5, 27.6, 26.6, 26.0, 21.2 ppm. Purity (HPLC): 95.4%. HRMS (m/z) $C_{50}H_{50}N_4O_{12}S$, $(M+H)^+$, calculated 931.32187, found 931.32079, error: 1.2 ppm.

Protease-Coupled PPIase assay

BpMip was transformed into BL21(DE3) cells and expressed and prepared as described [37]. **13** was tested in the protease-coupled PPIase assay according to a protocol by Vivoli et al. analogous to the other inhibitors studied [20]. The protease-coupled PPIase assay data for inhibitors **11, 15, 14**, and **2** were reported by Seufert et al., [18] PPIase data of **12** by Iwasaki et al. [3]

FP assay validation with BpMip and probe 1, thermodynamic study of the influence of temperature on K_D*, and ITC measurement*

BpMip was codon-optimized using an in-house script (available at https://github.com/njharmer/CodonOptimise) and the synthesized gene cloned into the pNIC28-Bsa4 vector (https://www.addgene.org/26103/) by Twist Bioscience. The BpMip-**1** interaction was measured following the methods of Rossi and Taylor [23]. 5 nM **1** was mixed with 15 concentrations of BpMip (200 mM to 12 nM in two-fold dilutions), or a buffer blank, in a buffer of 35 mM Hepes pH 7.8 in a 384 well black walled plate (Corning #3820) in a total volume of 40 μL. In the same plate, the same concentrations of BpMip in buffer alone, and with 5 nM **1** and 300 μM **11** were prepared to control for BpMip fluorescence and non-specific binding of **1** to BpMip. All samples were prepared in duplicate. Samples were incubated in the dark with mild shaking for 15 minutes, centrifuged at 300 *g* for two minutes, and incubated at 25°C for 20 minutes. Fluorescence anisotropy was measured using a Clariostar plate reader (BMG Labtech, Ortenberg, Germany) with excitation at 488 nm and emission at 518 nm. Gain optimization was performed using the manufacturer's recommendations. For measurements at different temperatures, the samples were incubated at the relevant temperature for 20 minutes before reading. A script was used to automate incubation and reading for samples and is available as a supplementary file. The raw parallel and perpendicular measurements were corrected for BpMip autofluorescence by subtracting the values of the paired BpMip only wells. Fluorescence anisotropy was calculated using Eq. (1):

$$A = \frac{(I_{\parallel} - I_{\perp})}{(I_{\parallel} + 2I_{\perp})} \tag{1}$$

where $I_{\parallel}$ and $I\perp$ are the parallel and perpendicular intensities, respectively.

Anisotropy due to non-specific binding was calculated at each protein concentration using Eq. (2):

$$A_{NS} = (A_I - A_D) * \left(1 - \frac{A_M - A_D}{A_{DR} - A_D}\right) \tag{2}$$

where A_{NS} is the non-specific anisotropy, A_M is the measured protein-**1** anisotropy at this concentration, A_I is the measured protein-**1** anisotropy in the presence of excess **11** at the relevant concentration, A_D is the anisotropy of **1** alone, and A_{DR} is the BpMip-**1** anisotropy at saturating BpMip. A_{NS} was subtracted from A_M at each concentration to give the final specific anisotropy A_s. The A_S values were fitted to the four-parameter ligand saturation (Eq. (3)):

$$A_S = lower + (upper - lower)\left(\frac{[BpMip]^h}{([BpMip]^h + EC_{50}^h)}\right) \tag{3}$$

where EC_{50} is the concentration of BpMip required to achieve a 50% effect, upper and lower are fully bound and unbound anisotropy of **1**, and *h* is the hill coefficient. As the EC_{50} is well in excess of the **1** concentration, EC_{50} is equivalent to K_D within error.

The van't Hoff plot was calculated by plotting the natural logarithm of K_D against the inverse of temperature (in Kelvin) and fitting a straight line with linear regression:

$$\ln K_D = \frac{\Delta H^o}{RT} + c \tag{4}$$

where R is the gas constant (8.314 J K^{-1} mol^{-1}). From the gradient of the line, ΔH° can be calculated. This then allows ΔS° to be calculated:

$$\Delta G^o = RT \ln K_D \tag{5}$$

$$\Delta G^o = \Delta H^o - T\Delta S^o \tag{6}$$

All calculations were performed in *R*. A script for performing these calculations is available as a supplementary file.

The determination of the G-factor was performed using the protocol provided by *Berthold Technologies* (Bad Wildbad, Germany) and resulted in a value of 1.15 for the instrument used.

FP was measured for the sensitivity study at 15 concentrations of **1** (0.005 nM to 50 nM) diluted in HEPES buffer (HEPES 20 mM, TritonX-100 0.002%, KCl 13.4 mM, pH 8).

For active site titration, tracer molecule **1** was mixed in equal parts to a final concentration of 5 nM with at least 8 concentrations of BpMip (100 µM to 0.05 nM, in different steps of dilution). For all experiments, the final volume in the 384 black, flat-bottom, non-binding well plates (*Greiner Bio-One*, Kremsmünster, Austria, #781900) was 60 µL. Incubation was performed for 30 min at room temperature in the dark, followed by measuring the FP value (Mithras LB 940, Berthold Technologies, Bad Wildbad, Germany) three times each well. The K_D value was calculated with GraphPad Prism 8.0.1 from Dotmatics (Boston, Massachusetts, USA) using the equation given by Wang et al. [47]

$$\Delta F = \frac{A/[L]_t}{2}\left\{\left([P]_t + [L]_t + K_D - \sqrt{([P]_t + [L]_t + K_D)^2 - 4[P]_t[L]_t}\right)\right\}$$

Fitting parameter:
ΔF = change in FP signal
A = FP amplitude, constant
L_t = total concentration of the ligand (tracer)
P_t = total concentration protein
K_D = dissociation constant

For the kinetics test, where the K_D value was determined over a period of 3 hours (0 min, 5 min, 15 min, 30 min, 1 h, 2 h and 3 h), the same procedure was followed as for active site titration. The experiment was carried out in duplicate and the incubation time of 30 min was maintained for all further experiments.

To examine the influence of DMSO, a mixture of a specific concentration of DMSO (0%, 0.5%, 1%, 2% and 4%) in HEPES buffer and the probe **1** (10 nM) was used in a total of 30 µL. After adding to 30 µL of BpMip (4 µM), resulting in a final concentration of 5 nM for **1**, 2 µM for BpMip and 0%, 0.25%, 0.5%, 1%, and 2% DMSO, respectively, and a total volume of 60 µL, FP was measured.

Negative control for Z-factor determination was therefore the same mixture as mentioned above with a final DMSO concentration of 0.5%,

which is the maximum of FP. For the minimum, the most potent inhibitor **12** in this series was chosen, diluted from DMSO stock to a final concentration of 150 μM of **12** and 0.5% DMSO (see SI).

The ITC measurement was performed by MicroCal iTC200 (*Danaher Corporation*, Washington, D.C., USA, formerly: **GE HealthCare**, Chicago, Illinois, USA). For this purpose, a stock solution of **1** was prepared at a concentration of 600 μM. Whereby the final DMSO concentration was 3%. Therefore, the measurement cell was filled with a 60 micromolar BpMip solution in HEPES buffer, which also contained 3% DMSO. After three measurements, the K_D value was 5.50 ± 0.03 μM. The FP assay gave a K_D of 3.6 μM for this DMSO concentration. Data were calculated using Origin 7 (*OriginLab Corporation*, Northampton, Massachusetts, USA).

Competitive displacement assay for the screening of BpMip inhibitors

To determine inhibitor K_i, stock DMSO solutions of each compound (approximately 25 mM) were prepared and then diluted with HEPES buffer in various dilution patterns (1:10; 1:5, 1:3). All competition assays were carried out as triplicates.

In the well, 15 μL inhibitor dilution (final concentrations from 50 μM to 2 nM) was mixed with 15 μL tracer (20 nM) as well as 30 μL BpMip (4 μM) to again obtain a final concentration of 5 nM **1** and 2 μM BpMip. To ensure the quality of the Mip protein before each measurement, a positive control consisting of BpMip (2 μM), probe **1** (20 nM), and buffer (in place of the competitor) was measured for each run. The constant binding affinity of the protein to the ligand is indicated by reaching the upper plateau of the mP values. This was interpreted as demonstrating the integrity of the Mip protein for that experiment.

Fitting parameter for the competition assay, according to Wang et al. [48]:

$$\Delta F = \frac{A\left\{2\sqrt{a^2-3b}\,\cos\left(\theta/3\right)-a\right\}}{3K_A+\left\{2\sqrt{a^2-3b}\,\cos\left(\theta/3\right)-a\right\}}+F_0$$

a=K_A+K_B+A_0+B_0-P_0 b=K_B*(A_0-P_0)+ K_A*(B_0-P_0)+ K_A*K_B c= -K_A*K_B*P_0 theta= arc cos((-2*a^3 + 9*a*b - 27*c)/(2*sqrt((sqr(a)-3b)^3)))

Y=Ampl*(2*sqrt(sqr(a)-3*b)*cos(theta/3)-a)/(3*K_A+(2*sqrt(sqr(a)-3*b)*cos(theta/3)-a))+Back

K_A= K_D of the tracer (ligand A)

K_B= K_i of the inhibitor (ligand B)

B_0= free inhibitor concentration

A_0= free tracer concentration

P_0= free protein concentration

F_0= FP signal minimum

Data were collected on two different instruments at the Universities of Würzburg and Exeter, giving similar results.

Author Contributions

‡ N.J.S. and T.L. are equal first authors, and U.H. and N.J.H. are equal corresponding authors.

N.J.S.: Formal analysis, Investigation, Writing – original draft, review & editing. T.L.: Formal analysis, Investigation, Methodology, Writing – original draft, review & editing. M.V.V.: Investigation, Methodology. F.S.: Investigation, Methodology. D.A.: Investigation. L.K..: Investigation. N.J.H: Conceptualization, Formal analysis, Funding acquisition, Investigation, Supervision, Validation, Writing – review & editing. U.H.: Conceptualization, Funding acquisition, Project Administration, Supervision, Validation, Writing – review & editing.

Supplementary Material

Supplementary data include NMR spectra and purity data of the tested compounds. The HRMS method and detailed K_D data are also provided. Further data and figures for assay validation and all replications with SEM of the competition assay are shown.

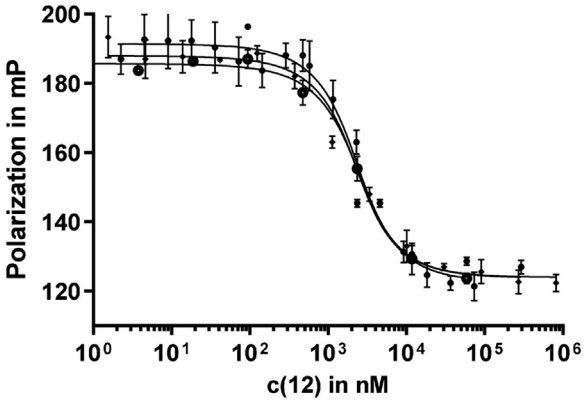

Fig. 6. Exemplary dose-response curve from competition assay performed with **12**. The triplicate measurement was performed on three different days with three different dilution series. 1 was used in a final concentration of 5 nM, BpMip at 2 μM and **12** in a range of 60 μM – 1 nM. GraphPad Prism 8.0.1 was used for calculation and graphical representation.

Declaration of Competing Interest

The authors declare that they have no known competing financial interests or personal relationships that could have appeared to influence the work reported in this paper.

Acknowledgments

Thanks are due to Ute Hellmich for providing purified BpMip. Felix Hausch is thanked for supporting data analysis with GraphPad. This work was supported by the North Atlantic Treaty Organization (NATO), Brussels, Belgium grant SPS 984835, and the German Research Foundation (DFG, Bonn, Germany; grant SFB 630) for the development of Mip inhibitors against *Legionella pneumophila* and *Burkholderia pseudomallei*, respectively, and The Federal Ministry of Education and Research (Germany, Berlin, project number 16GW0212 "iMIP") for the development of Mip inhibitors against *Trypanosoma cruzi* given to UH. This paper includes research that was supported by DMTC Limited (Australia, project number 10.44 "pharmaceutical development of antivirulence compounds against bio-warfare pathogens"), BBSRC grant BB/N001591/1, and UKRI CoA funds. The authors have prepared this paper in accordance with the intellectual property rights granted to partners from the original DMTC project.

Supplementary materials

Supplementary material associated with this article can be found, in the online version, at doi:10.1016/j.slasd.2023.03.004.

References

[1] Kohler R, Fanghanel J, Konig B, Luneberg E, Frosch M, Rahfeld JU, et al. Biochemical and functional analyses of the Mip protein: influence of the N-terminal half and of peptidylprolyl isomerase activity on the virulence of Legionella pneumophila. Infect Immun 2003;71(8):4389–97. doi:10.1128/IAI.71.8.4389-4397.2003.

[2] Norville IH, Harmer NJ, Harding SV, Fischer G, Keith KE, Brown KA, et al. A Burkholderia pseudomallei macrophage infectivity potentiator-like protein has rapamycin-inhibitable peptidylprolyl isomerase activity and pleiotropic effects on virulence. Infect Immun 2011;79(11):4299–307. doi:10.1128/IAI.00134-11.

[3] Iwasaki J, Lorimer DD, Vivoli-Vega M, Kibble EA, Peacock CS, Abendroth J, et al. Broad-spectrum in vitro activity of macrophage infectivity potentiator inhibitors against Gram-negative bacteria and Leishmania major. J Antimicrob Chemother 2022;77:1625–34. doi:10.1093/jac/dkac065.

[4] Scheuplein NJ, Bzdyl NM, Kibble EA, Lohr T, Holzgrabe U, Sarkar-Tyson M. Targeting protein folding: a novel approach for the treatment of pathogenic bacteria. J Med Chem 2020;63(22):13355–88. doi:10.1021/acs.jmedchem.0c00911.

[5] Rasch J, Unal CM, Klages A, Karsli U, Heinsohn N, Brouwer R, et al. Peptidyl-prolyl-cis/trans-isomerases Mip and PpiB of Legionella pneumophila contribute to surface translocation, growth at suboptimal temperature, and infection. Infect Immun 2019;87(1):e00939–17. doi:10.1128/IAI.00939-17.

[6] Leuzzi R, Serino L, Scarselli M, Savino S, Fontana MR, Monaci E, et al. Ng-MIP, a surface-exposed lipoprotein of Neisseria gonorrhoeae, has a peptidyl-prolyl cis/trans isomerase (PPIase) activity and is involved in persistence in macrophages. Mol Microbiol 2005;58(3):669–81. doi:10.1111/j.1365-2958.2005.04859.x.

[7] Lundemose AG, Kay JE, Pearce JH. Chlamydia trachomatis Mip-like protein has peptidylprolyl cis/trans isomerase activity that is inhibited by FK506 and rapamycin and is implicated in initiation of chlamydial infection. Mol Microbiol 1993;7(5):777–83. doi:10.1111/j.1365-2958.1993.tb01168.x.

[8] Unal CM, Steinert M. FKBPs in bacterial infections. Biochim Biophys Acta 2015;1850(10):2096–102. doi:10.1016/j.bbagen.2014.12.018.

[9] Moro A, Ruiz-Cabello F, Fernandez-Cano A, Stock RP, Gonzalez A. Secretion by Trypanosoma cruzi of a peptidyl-prolyl cis-trans isomerase involved in cell infection. EMBO J 1995;14(11):2483–90. doi:10.1002/j.1460-2075.1995.tb07245.x.

[10] Wiersinga WJ, Virk HS, Torres AG, Currie BJ, Peacock SJ, Dance DAB, et al. Melioidosis. Nat Rev Dis Primers 2018;4:17107. doi:10.1038/nrdp.2017.107.

[11] Birnie E, Virk HS, Savelkoel J, Spijker R, Bertherat E, Dance DAB, et al. Global burden of melioidosis in 2015: a systematic review and data synthesis. Lancet Infect Dis 2019;19(8):892–902. doi:10.1016/s1473-3099(19)30157-4.

[12] Norville, I. H.; Breitbach, K.; Eske-Pogodda, K.; Harmer, N. J.; Sarkar-Tyson, M.; Titball, R. W.; et al. A novel FK-506-binding-like protein that lacks peptidyl-prolyl isomerase activity is involved in intracellular infection and in vivo virulence of Burkholderia pseudomallei. Microbiology (Reading) 2011, 157 (Pt 9), 2629–38. DOI: 10.1099/mic.0.049163-0.

[13] Norville IH, O'Shea K, Sarkar-Tyson M, Zheng S, Titball RW, Varani G, et al. The structure of a Burkholderia pseudomallei immunophilin–inhibitor complex reveals new approaches to antimicrobial development. Biochem J 2011;437(3):413–22.

[14] Ceymann A, Horstmann M, Ehses P, Schweimer K, Paschke AK, Steinert M, et al. Solution structure of the Legionella pneumophila Mip-rapamycin complex. BMC Struct Biol 2008;8:17. doi:10.1186/1472-6807-8-17.

[15] Juli C, Sippel M, Jäger J, Thiele A, Weiwad M, Schweimer K, et al. Pipecolic acid derivatives as small-molecule inhibitors of the Legionella MIP protein. J Med Chem 2011;54(1):277–83. doi:10.1021/jm101156y.

[16] Begley DW, Fox D 3rd, Jenner D, Juli C, Pierce PG, Abendroth J, et al. A structural biology approach enables the development of antimicrobials targeting bacterial immunophilins. Antimicrob Agents Chemother 2014;58(3):1458–67. doi:10.1128/AAC.01875-13.

[17] Reimer A, Seufert F, Weiwad M, Ebert J, Bzdyl NM, Kahler CM, et al. Inhibitors of macrophage infectivity potentiator-like PPIases affect neisserial and chlamydial pathogenicity. Int J Antimicrob Agents 2016;48(4):401–8. doi:10.1016/j.ijantimicag.2016.06.020.

[18] Seufert F, Kuhn M, Hein M, Weiwad M, Vivoli M, Norville IH, et al. Development, synthesis and structure-activity-relationships of inhibitors of the macrophage infectivity potentiator (Mip) proteins of Legionella pneumophila and Burkholderia pseudomallei. Bioorg Med Chem 2016;24(21):5134–47. doi:10.1016/j.bmc.2016.08.025.

[19] Fischer G, Bang H, Mech C. Detection of enzyme catalysis for cis-trans-isomerization of peptide bonds using proline-containing peptides. Biomed Biochim Acta 1984;43(10):1101–11.

[20] Vivoli M, Renou J, Chevalier A, Norville IH, Diaz S, Juli C, et al. A miniaturized peptidyl-prolyl isomerase enzyme assay. Anal Biochem 2017;536:59–68. doi:10.1016/j.ab.2017.08.004.

[21] Mori T, Itami S, Yanagi T, Tatara Y, Takamiya M, Uchida T. Use of a real-time fluorescence monitoring system for high-throughput screening for prolyl isomerase inhibitors. J Biomol Screen 2009;14(4):419–24. doi:10.1177/1087057109333979.

[22] Owicki JC. Fluorescence polarization and anisotropy in high throughput screening: perspectives and primer. J Biomol Screen 2000;5(5):297–306. doi:10.1177/108705710000500501.

[23] Rossi AM, Taylor CW. Analysis of protein-ligand interactions by fluorescence polarization. Nat Protoc 2011;6(3):365–87. doi:10.1038/nprot.2011.305.

[24] Jameson DM, Ross JA. Fluorescence polarization/anisotropy in diagnostics and imaging. Chem Rev 2010;110(5):2685–708. doi:10.1021/cr900267p.

[25] Kozany C, Marz A, Kress C, Hausch F. Fluorescent probes to characterise FK506-binding proteins. ChemBioChem 2009;10(8):1402–10. doi:10.1002/cbic.200800806.

[26] Pomplun S, Sippel C, Hahle A, Tay D, Shima K, Klages A, et al. Chemogenomic profiling of human and microbial FK506-binding proteins. J Med Chem 2018;61(8):3660–73. doi:10.1021/acs.jmedchem.8b00137.

[27] Paulson CN, Guan X, Ayoub AM, Chan A, Karim RM, Pomerantz WCK, et al. Design, synthesis, and characterization of a fluorescence polarization Pan-BET bromodomain probe. ACS Med Chem Lett 2018;9(12):1223–9. doi:10.1021/acsmedchemlett.8b00380.

[28] Coons AH, Kaplan MH. Localization of antigen in tissue cells; improvements in a method for the detection of antigen by means of fluorescent antibody. J Exp Med 1950;91(1):1–13. doi:10.1084/jem.91.1.1.

[29] Kitano K, Schwartz DM, Zhou H, Gilpin SE, Wojtkiewicz GR, Ren X, et al. Bioengineering of functional human induced pluripotent stem cell-derived intestinal grafts. Nat Commun 2017;8(1):765. doi:10.1038/s41467-017-00779-y.

[30] Grimm JB, Heckman LM, Lavis LD. The chemistry of small-molecule fluorogenic probes. Prog Mol Biol Transl Sci 2013;113:1–34. doi:10.1016/B978-0-12-386932-6.00001-6.

[31] Magde D, Wong R, Seybold PG. Fluorescence quantum yields and their relation to lifetimes of rhodamine 6G and fluorescein in nine solvents: improved absolute standards for quantum yields. Photochem Photobiol 2007;75(4):327–34. doi:10.1562/0031-8655(2002)0750327fqyatr2.0.Co2.

[32] Banaszynski LA, Liu CW, Wandless TJ. Characterization of the FKBP center dot rapamycin, FRB ternary complex (vol 127, pg 4715, 2005). J Am Chem Soc 2006;128(49):15928. doi:10.1021/ja0699788.

[33] de Lorimier RM, Smith JJ, Dwyer MA, Looger LL, Sali KM, Paavola CD, et al. Construction of a fluorescent biosensor family. Protein Sci 2002;11(11):2655–75. doi:10.1110/ps.021860.

[34] Rinken A, Lavogina D, Kopanchuk S. Assays with detection of fluorescence anisotropy: challenges and possibilities for characterizing ligand binding to GPCRs. Trends Pharmacol Sci 2018;39(2):187–99. doi:10.1016/j.tips.2017.10.004.

[35] Moerke NJ. Fluorescence Polarization (FP) assays for monitoring peptide-protein or nucleic acid-protein binding. Curr Protoc Chem Biol 2009;1(1):1–15. doi:10.1002/9780470559277.ch090102.

[36] Huang X, Aulabaugh A. Application of fluorescence polarization in HTS assays. Methods Mol Biol 2016;1439:115–30. doi:10.1007/978-1-4939-3673-1_7.

[37] Norville IH, O'Shea K, Sarkar-Tyson M, Zheng S, Titball RW, Varani G, et al. The structure of a Burkholderia pseudomallei immunophilin-inhibitor complex reveals new approaches to antimicrobial development. Biochem J 2011;437(3):413–22. doi:10.1042/BJ20110345.

[38] Tjernberg A, Markova N, Griffiths WJ, Hallen D. DMSO-related effects in protein characterization. J Biomol Screen 2006;11(2):131–7. doi:10.1177/1087057105284218.

[39] Eastwood BJ, Farmen MW, Iversen PW, Craft TJ, Smallwood JK, Garbison KE, et al. The minimum significant ratio: a statistical parameter to characterize the reproducibility of potency estimates from concentration-response assays and estimation by replicate-experiment studies. J Biomol Screen 2006;11(3):253–61. doi:10.1177/1087057105285611.

[40] Wildey, M. J.; Haunso, A.; Tudor, M.; Webb, M.; Connick, J. H. Chapter five - high-throughput screening. In Annual reports in medicinal chemistry, Goodnow, R. A. Ed.; Vol. 50, 149-195; Academic Press, 2017.

[41] Zhang JH, Chung TD, Oldenburg KR. A simple statistical parameter for use in evaluation and validation of high throughput screening assays. J Biomol Screen 1999;4(2):67–73. doi:10.1177/108705719900400206.

[42] Hünig S, K P, Märkl G, Sauer J. Arbeitsmethoden in der organischen chemie. Berlin: Lehmanns Verlag; 2006.

[43] Fulmer GR, Miller AJM, Sherden NH, Gottlieb HE, Nudelman A, Stoltz BM, et al. NMR chemical shifts of trace impurities: common laboratory solvents, organics, and gases in deuterated solvents relevant to the organometallic chemist. Organometallics 2010;29(9):2176–9. doi:10.1021/om100106e.

[44] Baer, T.; Beckers, T.; Gekeler, V.; Gimmnich, P.; Joshi, H.; Joshi, U.; et al., inventors; 4SC AG, GE, assignee. Novel Tetrahydrofusedpyridines as histone deacetylase inhibitors. International patent, International publication number WO2009037001A4. 2009 Mar 26.

[45] Lameijer LN, Ernst D, Hopkins SL, Meijer MS, Askes SHC, Le Devedec SE, et al. A red-light-activated ruthenium-caged NAMPT inhibitor remains phototoxic in hypoxic cancer cells. Angew Chem Int Ed Engl 2017;56(38):11549–53. doi:10.1002/anie.201703890.

[46] Beutel, B. A.; Dandliker, P. J.; Hale, S. P.; Murcko, M. A.; Boczek, E.; Mittasch, M.; et al., inventors; Dewpoint Therapeutics, Inc., USA, assignee. Methods of characterizing condensate-associated characteristics of compounds and uses thereof. International Patent, international publication number WO2020163795A1, 2020 Aug 13.

[47] Wang Z-X, Ravi Kumar N, Srivastava DK. A novel spectroscopic titration method for determining the dissociation constant and stoichiometry of protein-ligand complex. Anal Biochem 1992;206(2):376–81. doi:10.1016/0003-2697(92)90381-g.

[48] Wang Z-X. An exact mathematical expression for describing competitive binding of two different ligands to a protein molecule. FEBS Lett 1995;360(2):111–14. doi:10.1016/0014-5793(95)00062-e.